Desalination and Water Treatment
www.deswater.com

doi:10.5004/dwt.2019.23479

141 (2019) 331–341
February

Adsorptive removal of azo dye in a continuous column operation using biosorbent based on NaOH and surfactant activation of *Prunus dulcis* leaves

Suyog N. Jain, Parag R. Gogate*

Chemical Engineering Department, Institute of Chemical Technology, Nathalal Parekh Marg, Matunga, Mumbai 400019, India, email: snjain@kkwagh.edu.in (S. Jain), Tel. +91 22 33612024, Fax +91 22 33611020, email: pr.gogate@ictmumbai.edu.in (P.R. Gogate),

Received 20 July 2018; Accepted 17 November 2018

ABSTRACT

The adsorption of Acid Blue 113, an azo dye, from aqueous solution using biosorbent obtained from NaOH and surfactant activation of waste biomass of *Prunus dulcis* has been studied in the present work in column operation. The effect of various operating conditions as depth of biosorbent in the bed, influent concentration, flow rate and salt concentration on the extent of adsorption and the breakthrough characteristics have been investigated. The obtained breakthrough data was applied to different models to check the fitting using linear and nonlinear regression analysis also obtaining the model parameters for best fitting models. Error analysis using root mean square error function was performed to predict the best model fitting in terms of matching experimental values to model predicted values, closer values of correlation coefficient to unity and least error values. Yoon Nelson and Thomas models were found to be in better agreement to the obtained breakthrough data. Maximum uptake capacity was established as 59.54 mg/g for the operation with 100 mg/L as the influent dye concentration at the established optimum flow rate of 6 mL/min. Desorption and subsequent re-usability studies conducted for three cycles using ethanol as the desorbing agent confirmed the effectiveness of synthesized biosorbent for dye removal in multiple cycles as only slight decrease in biosorption capacity was observed from 52.50 mg/g for first cycle to 49.42 mg/g for third cycle of reuse. Extent of elution (%) was also found to marginally decrease from 98.59% for first cycle to 83.81% for third cycle of reuse. Overall, the column study clearly established that synthesized biosorbent is a promising adsorbent to treat Acid Blue 113 containing dye effluent in a continuous operation.

Keywords: Acid Blue 113 adsorption; Azo dye; *Prunus dulcis*; Column study; Regeneration

1. Introduction

Rapid growth in industrialization and population has also resulted in significant contamination of water with various pollutants as metals, dyes, etc. Synthetic dyes, especially azo dyes, are commonly used to color products in textile, dyestuff, paper and plastic industries. Azo dyes typically constitute to 70% of the total synthetic dyes being used in the different industries [1,2]. Annually, about 1 million tons of azo dyes are manufactured and around 2000 different types of azo dyes are being used for different industrial applications [3]. Azo dyes are preferred in garment and textile industries due to their ease in application, availability in variety of brilliant shades and capacity of strong attachment to fibers [4]. Even though azo dyes are having significant properties suitable for wide spread application, there are associated problems especially when it comes to treatment of effluent containing azo dyes. Azo dyes are recalcitrant, offer resistance to aerobic digestion, are stable towards oxidizing agents and also can be quickly broken down to amines, which are more toxic and can cause serious environmental hazards [5,6]. High molecular weight and complex structure of azo dyes typically make them difficult to mineralize [7]. During the process of dyeing, significant amount of azo dyes are lost in the wastewater, which creates pollution and can disturb the equilibrium of flora and fauna [8]. Considering this analysis, research into developing effective methodology

*Corresponding author.

for the removal of azo dyes is very important. The present work focuses on Acid Blue 113 dye which is an important compound belonging to the class of azo dyes. Chemical structure of Acid Blue 113 is based on aromatic rings and azo group, which are contributing to the non-biodegradable and toxic nature [9]. The discharge of acid blue 113 bearing effluent can reduce transparency of water and hence rate of transfer of oxygen into water, which affects photosynthesis of aquatic system [10]. Hence treatment of effluent containing acid blue 113 is very important to avoid serious environmental concern. It is also necessary to mineralize the dye present in the wastewater and reuse the water as clean water resources may get depleted in coming years. Developing the efficient techniques to remove the azo dye from wastewater would be thus of great benefit to the environment and hence the importance of current work is clearly established.

Typically, effluent containing azo dyes is treated using different techniques as photocatalysis [11], coagulation [12], ozonation [13], ultrafiltration membrane separation [14], oxidation [15], and electrochemical destruction [16]. Most of these treatment techniques have their own advantages however they also suffer from severe drawbacks as significantly higher process cost, lower efficacy, sludge formation, possibility of harmful by-products, limitations on commercialization, etc. [17,18]. In compared to all these reported techniques, adsorption is attractive technique to treat dye effluents due to its simplicity and effectiveness. In the process of adsorption, the widely applied adsorbent for treatment of dye effluents is activated carbon due to its significant porosity and surface area. But the limitations as higher cost of activated carbon and requirement of high pressure steam for regeneration leads to overall increase in the cost of the operation [19,20]. The drawbacks associated with activated carbon have motivated research community to search for other substrates as an alternate to activated carbon. Sustainable biomass has drawn significant attention as a substrate for adsorbent synthesis and subsequent application for control of pollution. Considering the easy availability and low cost of substrate as an adsorbent for azo dye removal, researchers have tried different adsorbents in native form as waste of fish scales [21], peels of *Cucumis sativus* [22], lady's finger [23], natural serpentine [24], in the native form and also in modified form as calcium titanate from egg shells and TiO_2 [25], H_2SO_4 activated charcoal ash [26], nanocomposites prepared using polymerization method [27], $ZnCl_2$ modified grape waste [28] etc.

In the present study, synthesis of biosorbent was performed from fallen (dead) leaves of almond (*Prunus dulcis*) with NaOH and surfactant activation for enhancing the activity toward adsorption. Almond fallen leaves are available in large quantity throughout the world and specifically in India. The application of such waste biomass for synthesis of biosorbent can also serve the purpose of solid waste management. In our earlier work [29], NaOH and surfactant activated *Prunus dulcis* (PD) was applied for treatment of Acid Blue 113 containing wastewater in batch operation. Typically, in batch operations, small volumes of dye effluents are effectively treated though industrial effluent consists of large volumes of the wastewater, which necessitates the use of continuous operation [30,31]. Continuous operation of adsorption are typically conducted in fixed beds due to ease in operation and minimum loss of the adsorbent during the operation [32]. Hence in the present work, continuous operation has been investigated using fixed bed column. Detailed literature survey revealed that not many reports for Acid Blue 113 dye removal in a continuous column operation are available in the literature and only one preliminary investigation could be found. Gupta et al. [33] reported the studies for establishing the breakthrough capacity of the column for Acid Blue 113 removal using rubber tire activated carbon however the detailed column study related to effect of column parameters on breakthrough parameters was not reported. Desorption study was conducted using NaOH solution as an eluent but the recovered adsorbent was not subjected again for adsorption studies to check the re-usability. Also, the literature survey revealed that the application of dead leaves of *Prunus dulcis* in a continuous mode of operation has not been reported in any study and hence, the present study in terms of exploring the use of biosorbent obtained from *Prunus dulcis* for Acid Blue 113 removal in a fixed bed operation is novel. The objective of the present work is to investigate the potential of synthesized NaOH and surfactant activated biosorbent for Acid Blue 113 removal from simulated wastewater in a continuous operation, which is a very important study considering the possible commercial scale application. The effects of operating parameters on the efficacy of dye removal have been investigated to establish the breakthrough conditions. The performance of the column has been analyzed from the established breakthrough curves based on different adsorption column models. Error analysis has also been performed to establish the best model fitting to the experimentally obtained breakthrough data. Re-usability study has also been conducted by removing the dye from dye loaded biosorbent using ethanol applied as the desorbing agent and subsequently activating the obtained biosorbent using thermal activation. Recovered biosorbent has been again subjected to adsorption studies in three cycles for checking the efficacy for reuse. Such type of re-usability studies in continuous operation have also not been reported in the literature for the biosorbent based on dead leaves of *Prunus dulcis*, which again confirms the novelty of the present work in terms of reusability studies.

2. Materials and methods

2.1. Materials

Fallen (dead) leaves of PD used in the present work were collected from Nashik. Acid Blue 113 dye, pollutant in the present work was procured from Sigma-Aldrich, Mumbai. Stock solution of Acid Blue 113 dye with strength of 1 g/L was prepared initially and the working solutions of required concentrations were subsequently prepared by diluting the stock solution with distilled water.

2.2. Biosorbent synthesis and characterization

Collected leaves were washed, air dried, powdered and sieved. Powder was then activated in oven at 60°C for 4 h and treated with 1% solution of NaOH. The NaOH activated powder was filtered, washed and further activated in oven overnight. NaOH activated PD biosorbent further activated using cetyl trimetyl ammonium bromide (CTAB) treatment by adding NaOH activated PD biosorbent in 1% CTAB solution. The solution was then stirred in orbital shaker (Bio-Technics,

India) at the speed of 100 rpm for 12 h. The solution was subsequently filtered, washed and dried. The obtained surfactant modified PD biosorbent (described as SMPD) in this process was then kept in dessicator for column studies. Details of characterization performed using BET, SEM, FTIR and elemental analysis has been described in our earlier work [29].

2.3. Quantification of pollutant

Spectrum of Acid Blue 113 dye absorption over different scanning wavelengths was obtained using Ultra Violet (UV)-visible spectrophotometer (UV 1800, Shimadzu). Maximum wavelength of UV absorption, λ_{max} for the Acid Blue 113 dye was established as 566 nm. Calibration chart was then prepared based on the analysis of Acid Blue 113 dye solutions of known concentrations. The chart was then used to quantify the dye remaining in the treated solutions after the adsorption studies.

2.4. Experimental methodology

Continuous studies were conducted in a column of 2 cm diameter, packed with the known biosorbent quantity up to the desired biosorbent bed depth. At the top and the bottom of the bed, glass wool was provided so as to ensure no loss of the biosorbent from the bed during the adsorption. Glass beads were also provided to support the fixed bed in the column. Peristaltic pump (Ravel Hiteks, Chennai) equipped with variable speed knob was used to pass the Acid Blue 113 solution through the biosorbent bed in the upward direction. The effect of important operating parameters as bed depth (Z), influent concentration (C_i), flow rate (F) and salt concentration on the efficacy of Acid Blue 113 removal have been studied. The collected dye samples from the top of the column at particular operating condition were centrifuged using centrifuge (Remi Scientific Works, Mumbai) to remove fine particles (if any) from the residual solutions. Residual concentration of Acid Blue 113 in supernatant samples (C_t) were then determined using spectrophotometer and the established calibration chart. Experimental data were subjected to different column models and error analysis was performed to check fitting of the breakthrough data to the applied models. Desorption and subsequent re-usability studies have also been conducted for three cycles using ethanol as an eluent [34].

2.5. Analysis of column data

Breakthrough curves have been plotted to understand the column performance based on different design parameters. The breakthrough time (t_b) is the time at which concentration of dye in the exit stream (C_t) is 0.1 times the influent concentration (C_i) [35]. Exhaustion (saturation) time (t_{eff}) is the time at which column is said to be exhausted and is determined mathematically when concentration of dye in exit stream is 0.9 times influent concentration [36]. Effluent volume, V_{eff} (mL) collected at saturation of the column was also determined as given below [37]:

$$V_{eff} = Ft_{eff} \tag{1}$$

where F is volumetric flow rate of dye solution through the bed (mL/min).

Dye adsorbed in the bed, m_{ad} (mg) after the complete operation was determined using the equation as given below [38]:

$$m_{ad} = \frac{F}{1000}\int_{t=0}^{t=t_{total}} C_{ad}dt \tag{2}$$

where C_{ad} is the concentration of adsorbed dye (mg/L) determined on the basis of influent concentration and concentration in the outlet stream and t_{total} is total operation time (min).

Equilibrium biosorption capacity (q_{eq}) was calculated using the equation as given below [39]:

$$q_{eq} = \frac{m_{ad}}{W} \tag{3}$$

where W is adsorbent mass (g) in the bed.

Empty bed contact time (EBCT) is the time of contact between the biosorbent bed and the dye. EBCT was determined using the equation as given below [40]:

$$EBCT = \frac{V_B}{F} \tag{4}$$

where V_B is bed volume (mL).

Extent of desorption (%), defined as mass of dye desorbed (m_{de}) to mass of dye adsorbed (m_{ad}) expressed in terms of percentage was calculated using the equation as given below [41]:

$$Desorption(\%) = \frac{m_{de}}{m_{ad}} \times 100 \tag{5}$$

2.6. Modeling of breakthrough curves

Different models have been developed to predict the column adsorption study. In the present work, the different models applied to the obtained data include Bohart-Adams model, Thomas model and the Yoon-Nelson model.

2.6.1. Bohart-Adams model

Bohart-Adams model assumes that adsorption rate is proportional to remaining uptake capacity of the adsorbent and concentration of adsorbate.

Model in nonlinear form [42] is expressed by the following equation:

$$\frac{C_t}{C_i} = \exp\left(k_{BA}C_i t - \frac{k_{BA}N_0 H}{U_0}\right) \tag{6}$$

Model in linear form is expressed by the following equation:

$$\ln\left(\frac{C_t}{C_i}\right) = k_{BA}C_i t - k_{BA}N_0\frac{H}{U_0} \tag{7}$$

where k_{BA} is model constant (L mg^{-1} min^{-1}), N_0 is maximum uptake capacity (mg/L), H is depth of biosorbent in the bed (cm) and U_0 is linear velocity through the bed (cm/min).

2.6.2. Thomas model

Thomas model assumes that adsorption follows Langmuir kinetics with negligible axial dispersion in continuous column. Model in nonlinear form [43] is expressed by the following equation:

$$\frac{C_t}{C_i} = \frac{1}{1+\exp\left(\frac{k_{Th}q_{Th}W}{F} - k_{Th}C_i t\right)} \tag{8}$$

Model in linear form is expressed by the following equation:

$$\ln\left(\frac{C_i}{C_t} - 1\right) = \frac{k_{Th}q_{Th}W}{F} - k_{Th}C_i t \tag{9}$$

where k_{Th} is constant of model (mL min^{-1} mg^{-1}) and q_{Th} is maximum uptake capacity (mg/g).

2.6.3. Yoon-Nelson model

Yoon-Nelson model assumes that rate of decrease in the adsorption of individual molecule of adsorbate is proportional to probability of adsorption of adsorbate and the probability of breakthrough of adsorbate on the adsorbent. The Yoon-Nelson model in nonlinear form [44] is expressed by the following equation:

$$\frac{C_t}{C_i - C_t} = \exp\left(k_{YN}t - \tau k_{YN}\right) \tag{10}$$

Model in linear form is expressed by the following equation:

$$\ln\left(\frac{C_t}{C_i - C_t}\right) = k_{YN}t - \tau k_{YN} \tag{11}$$

where k_{YN} is constant of Yoon-Nelson model (min^{-1}) and τ is time (min) necessary for 50% breakthrough.

2.7. Error analysis

To find the best fitting model to the breakthrough data, root mean square error function (*RMSE*) [45] was used. *RMSE* values were determined using the following equation:

$$RMSE = \sqrt{\frac{1}{N}\Sigma\left[\left(\frac{C_t}{C_i}\right)_{pred} - \left(\frac{C_t}{C_i}\right)_{\exp}\right]^2} \tag{12}$$

where $(C_t/C_i)_{pred}$ is the ratio of exit to inlet dye concentration, calculated using model equations and $(C_t/C_i)_{exp}$ is the ratio of exit to inlet dye concentration, obtained experimentally. N is number of experimental observations.

3. Results and discussion

3.1. Characterization and possible mechanism of adsorption

In the present work, dead leaves of PD have been activated initially by NaOH treatment and then by CTAB treatment. Dead leaves of PD contain lignin, which blocks the pores and can offer resistance to the dye adsorption. Applied NaOH treatment was with an objective of removing the lignin and thus making the pores open for dye adsorption. Surface area of raw PD obtained as 67.02 m^2/g significantly increased to 426.35 m^2/g due to NaOH activation confirming the opening of the structure and removal of lignin. The NaOH activated biosorbent was further activated using CTAB treatment. The targeted pollutant in the present work is Acid Blue 113 dye, which is anionic in nature. Anionic dye removal can be enhanced if cationic charge is developed on the biosorbent as dominant electrostatic attractions will exist [46]. Hence CTAB, which is a cationic in nature, was used for activation. It was observed that surface area of NaOH treated PD obtained as 426.35 m^2/g reduced to 243.64 m^2/g due to applied CTAB treatment possibly due to the incorporation of CTAB. However the main objective was to alter the surface chemistry of the biosorbent and hence CTAB treated biosorbent was used in the study. Cationic head of the surfactant on the SMPD exterior surface can be responsible for the adsorption of anionic Acid Blue 113 dye. Electrostatic attraction existing between cationic head of CTAB and anionic group (SO_3^-) of Acid Blue 113 can enhance the dye adsorption on SMPD. Additionally, van der Waals forces of interaction between CH_2 group of biosorbent and Acid Blue 113 phenyl ring also contribute to the favored Acid Blue 113 adsorption. A detailed discussion on the results of BET, FTIR to establish the different surface groups and elemental analysis to confirm the incorporation of active groups have already been described in our earlier work [29].

3.2. Effect of biosorbent bed depth (H)

The obtained breakthrough curves (C_t/C_i vs. t) at varying bed depths of 3 cm (2.28 g loading of biosorbent), 4 cm (3.04 g loading of biosorbent) and 5 cm (3.8 g loading of biosorbent) at constant operating conditions of flow rate as 8 mL/min and influent concentration as 100 mg/L are shown in Fig. 1. The established breakthrough parameters are listed in Table

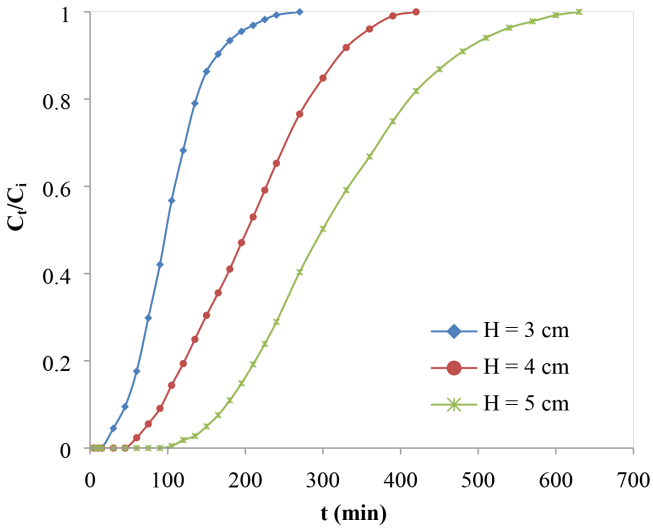

Fig. 1. Effect of biosorbent bed depth on breakthrough curves for biosorption of Acid Blue 113 dye on SMPD (C_i = 100 mg/L, F = 8 mL/min).

1. As seen from Fig. 1, breakthrough curves are more gradual at increased bed depths indicating that more time is required for saturation at higher depths [47]. As seen from Table 1, exhaustion time (t_{eff}) and effluent volume (V_{eff}) increased with an increase in bed depth. Increase in exhaustion time is attributed to availability of more surface area due to the higher available quantum of biosorbent at higher biosorbent depths [48]. More exhaustion time indicates better biosorption capacity. Biosorption capacity was also observed to increase from 34.18 mg/g at 3 cm to 65.04 mg/g at 5 cm of bed depth. The observed trend can be attributed to the fact that at higher bed depths, more amount of biosorbent and hence more biosorption sites and EBCT are available for adsorption of Acid Blue 113 molecules on SMPD surface [49] leading to higher extents of adsorption. Similar trend has also been reported for basic blue 3 removal using sugarcane bagasse [50].

3.3. Effect of influent dye concentration (C_i)

The obtained breakthrough curves (C_t/C_i vs. t) at varying influent dye concentrations over the range of 50–200 mg/L at constant operating conditions as bed depth of 4 cm and flow rate as 8 mL/min are depicted in Fig. 2. The established breakthrough parameters for this set of operation are also given in Table 1. As seen from Fig. 2, the breakthrough curves are flat at lower influent concentration and shift to left at higher influent concentration indicating less exhaustion time (t_e) and hence faster saturation of the bed occurring at increased influent concentrations. The observed trend can be due to faster filling of biosorption sites and an increase in driving force at higher dye concentration. At higher influent concentration, enhanced input of dye led to faster saturation of the bed and early occurrence of breakthrough. In other words, at higher concentration, the concentration gradient is higher, so that the mass transfer rate is higher which means that breakthrough occurred early [51]. The biosorption capacity was found to increase from 37.02 mg/g at lower influent concentration as 50 mg/L to 68.46 mg/g at higher influent concentration as 200 mg/L. The observed trend of increase in biosorption capacity can be explained on the basis of increased driving force for the transfer of molecules at higher dye concentration to overcome the associated mass transfer resistance [52]. Similar trend of higher biosorption capacity at increased influent dye concentration was also reported for methylene blue removal using watermelon rind based biosorbent [53].

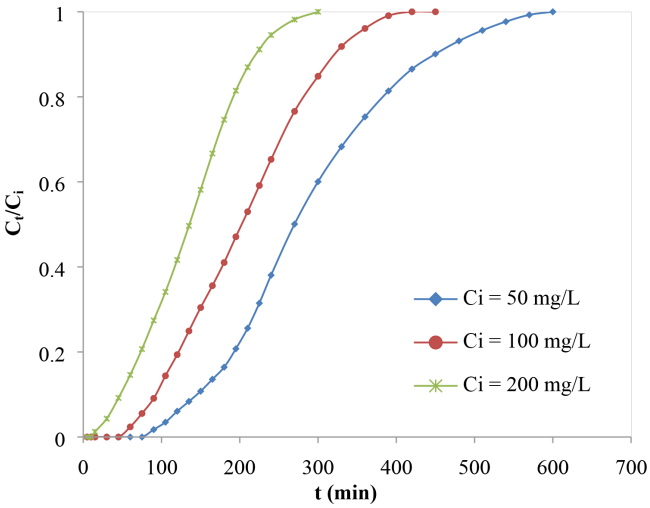

Fig. 2. Effect of influent dye concentration on breakthrough curves for biosorption of Acid Blue 113 dye on SMPD (H = 4 cm, F = 8 mL/min).

3.4. Effect of flow rate (F)

The breakthrough curves (C_t/C_i vs. t) at varying flow rates of 6, 8 and 10 mL/min at constant operating conditions as bed depth of 4 cm and influent dye concentration as 100 mg/L are illustrated in Fig. 3. The established breakthrough parameters for this set of operation at varying flow rates are listed in Table 1. The breakthrough curves are again found to be flat at lower flow rates and shift to left with an increase in the flow rate of dye solution indicating less exhaustion time (t_e) and hence faster saturation of the bed occurring at higher flow rates [54]. It can be seen from Table 1 that EBCT, breakthrough time (t_b) and effluent volume (V_e) decreased with an increase in flow rate of dye solution. The biosorption capacity was found to decrease from 59.54 mg/g at 6 mL/min to 43.45 mg/g at 10 mL/min as the flow rate. The observed trends can be attributed to the fact that at higher flow rates, solution moves faster along the column, reducing the available contact time for adsorption of dye [55]. Also, increase in flow rate increases the driving force for adsorption and quickly ensures the supply of new dye molecules leading to early saturation of the bed and breakthrough is achieved quickly. At lower flow rates, dye molecules remain in the biosorbent bed for longer time leading to more contact between molecules and

Table 1
Column data and breakthrough parameters for operations at different biosorbent bed depth (H), influent dye concentration (C_i) and flow rate (F) for removal of Acid Blue 113 dye using SMPD

H (cm)	C_i (mg/L)	F (mL/min)	t_b (min)	EBCT (min)	$t_{0.5}$ (min)	t_{eff} (min)	V_{eff} (L)	q_{eq} (mg/g)
3	100	8	45	1.18	95	165	1.32	34.18
4	100	8	95	1.57	205	325	2.56	52.50
5	100	8	175	1.96	300	480	3.84	65.04
4	50	8	145	1.57	270	450	3.60	37.02
4	200	8	50	1.57	135	220	1.76	68.46
4	100	6	165	2.09	290	475	2.85	59.54
4	100	10	60	1.26	135	215	2.15	43.45

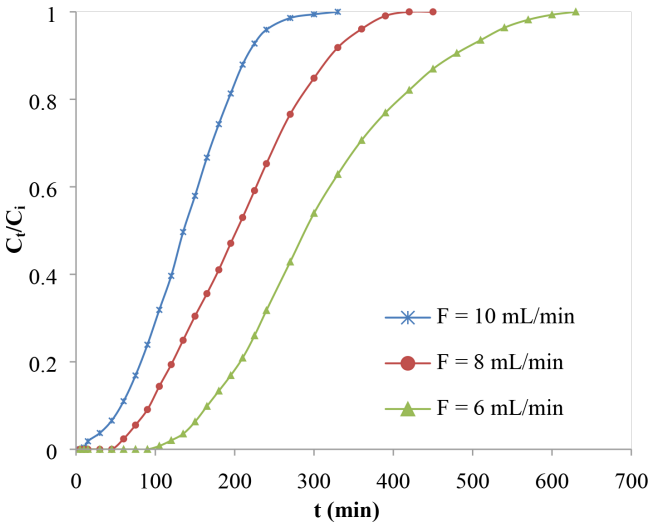

Fig. 3. Effect of flow rate of dye solution on breakthrough curves for biosorption of Acid Blue 113 dye on SMPD (H = 4 cm, C_i = 100 mg/L).

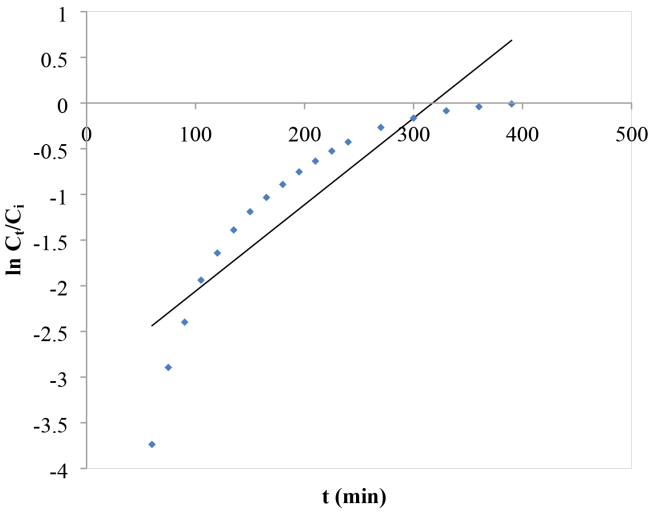

Fig. 4. Bohart-Adams plot for the removal of Acid Blue 113 dye using SMPD biosorbent (H = 4 cm, C_i = 100 mg/L, F = 8 mL/min).

biosorbent surface and hence higher biosorption capacity is obtained at lower flow rates yielding better column performance at lower flow rates [56]. Similar trend of higher uptake capacities at lower flow rate was also reported for methylene blue adsorption on rice husk [57]. Considering the analysis it can be said that an optimum flow rate needs to be selected for the treatment of wastewater using fixed bed column which can give both complete utilization of the adsorbent capacity as well as better mass transfer rates and the treatment time.

3.5. Effect of concentration of salt

Effluent from the dye industry also contains salts, which is likely to affect adsorption of dye on the adsorbent. To check the influence of the salts on the efficacy of the dye removal, in the present work, NaCl salt at concentration of 0.1 mol/L was added in the Acid Blue 113 dye solution having 100 mg/L as the initial concentration. The dye solution containing the salt was then passed at flow rate of 8 mL/min through the column packed with biosorbent at 4 cm depth and obtained results from the breakthrough data were compared with the dye solution without salt under similar operating conditions. It was observed that obtained biosorption capacity (52.5 mg/g) in the absence of salt was reduced marginally to 49.91 mg/g in the presence of salt at 0.1 mol/L concentration. Salt anion may compete with the dye anion for adsorption on cationic biosorbent surface leading to decrease in biosorption capacity. Similar results were also reported for adsorption of methyl orange using activated hydrochar [58].

3.6. Fitting of different models to breakthrough curves

The obtained data of breakthrough were subjected to model fitting using linear and nonlinear regression.

3.6.1. Bohart-Adams model

Bohart-Adams model in linear form was applied to the column data as depicted in Fig. 4 (plot of ln (C_t/C_i) vs. t) and the obtained model parameters, k_{BA} from slope and N_0 from intercept of Fig. 4 as well as the correlation coefficient and R^2 values are given in Table 2. The obtained model parameters using nonlinear regression are also listed in Table 2. The obtained values of N_0 using both regressions were observed to increase with an increase in bed depth whereas k_{BA} values were observed to decrease. The trends can be attributed to an increase in retention time of dye in the bed at increased depths, leading to increase in adsorption capacities (N_0) and decrease in kinetic constants (k_{BA}). Lower values of k_{BA} at increased depths indicated that overall kinetics of the adsorption was dominated by external mass transfer in the initial part in the fixed bed [59]. Similar trend of higher N_0 and lower k_{BA} values at higher bed depths was also reported for the removal of denim blue using inorganic adsorbents [60]. Though the trends were similar, it was also observed that R^2 values obtained using linear regression (average value of 0.7640) and nonlinear regression (average value of 0.8155) are not closer to 1 and Error *(RMSE)* values are quite high for all the column parameter studies indicating that Bohart-Adams model did not fit well to the column data. Due to these observations, it can be said that analysis of regression coefficients is important and only trend matching should be avoided.

3.6.2. Thomas model

Thomas model in linear form was also applied to the column data as depicted in Fig. 5 (plot of ln [$(C_i/C_t) - 1$] vs. t) and obtained model parameters, k_{Th} from slope and q_{Th} from the intercept of curve presented in Fig. 5 and R^2 values are depicted in Table 3. The obtained model parameters using nonlinear regression are also listed in Table 3. q_{Th} values using both regressions were found to be higher at higher bed depth and influent concentration whereas q_{Th} values were found to be lower at higher values of flow rates. Lower q_{Th} values at higher values of flow rates can be due to insufficient retention time in the column causing incomplete diffusion of Acid Blue 113 into cavities of SMPD biosorbent, and hence lower q_{Th} values

Table 2
Bohart-Adams model parameters for the removal of Acid Blue 113 dye using SMPD

Column parameters	H (cm)	3	4	5	4	4	4	4
	C_i (mg/L)	100	100	100	50	200	100	100
	F (mL/min)	8	8	8	8	8	6	10
Linear regression	k_{BA} (L mg^{-1} min^{-1})	0.00013	0.00010	0.00008	0.00014	0.00007	0.00008	0.00016
	$N_0 \times 10^{-3}$ (mg/L)	16.35	20.14	24.67	14.78	27.42	23.16	17.82
	R^2	0.7511	0.7868	0.7331	0.7881	0.7945	0.7323	0.7621
	RMSE	0.2816	0.4283	0.3916	0.4220	0.3154	0.3539	0.5783
Nonlinear regression	k_{BA} (L mg^{-1} min^{-1})	0.00006	0.00005	0.00004	0.00008	0.00003	0.00004	0.00006
	$N_0 \times 10^{-3}$ (mg/L)	19.32	23.55	28.98	15.79	34.23	26.98	22.24
	R^2	0.7585	0.8535	0.8432	0.7886	0.8336	0.8374	0.7927
	RMSE	0.1939	0.1364	0.1542	0.1764	0.1464	0.1571	0.1710

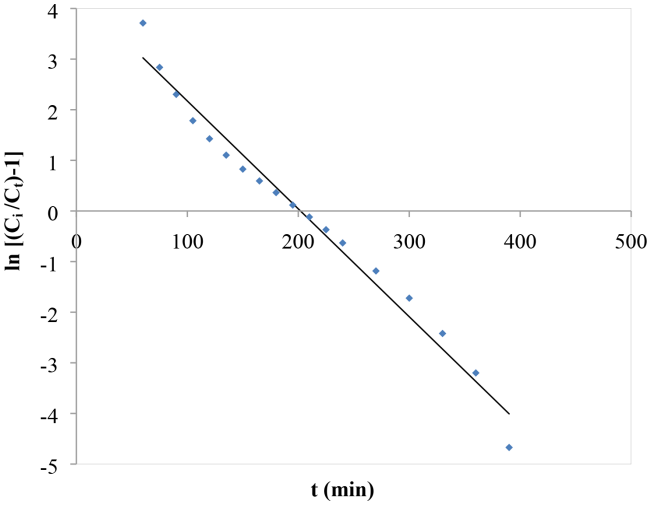

Fig. 5. Thomas plot for the removal of Acid Blue 113 dye using SMPD biosorbent (H = 4 cm, C_i = 100 mg/L, F = 8 mL/min).

are obtained. Similar trend of lower q_{Th} values at higher values of flow rates was also reported for methylene blue adsorption on *Eucalyptus sheathiana* barks [61]. R^2 values obtained using linear regression (average value of 0.9772) and nonlinear regression (average value of 0.9967) for the Thomas model are quite close to unity. R^2 values obtained using nonlinear regressions were found to be quite closer to unity in comparison with linear regression. Experimental values of maximum uptake capacity (q_{eq}) and uptake capacity values predicted using Thomas model (q_{Th}) were also found to be close to each other for all the studied column parameters for both regressions. Again q_{eq} and q_{Th} were found to be comparatively closer to each other for nonlinear regression than linear regression indicating better predictions based on non-linear regression. Error values calculated by Thomas model were also very less as seen from Table 3. All these findings confirmed that obtained column data suitably fitted to the Thomas model. Similar fitting of Thomas model has also been reported for removal of orange G dye using polymeric adsorbent [62].

Table 3
Thomas model parameters for the removal of Acid Blue 113 dye using SMPD

Column parameters	H (cm)	3	4	5	4	4	4	4
	C_i (mg/L)	100	100	100	50	200	100	100
	F (mL/min)	8	8	8	8	8	6	10
Linear regression	k_{Th} (mL min^{-1} mg^{-1})	0.352	0.213	0.168	0.316	0.141	0.163	0.316
	q_{Th} (mg/g)	36.43	53.17	68.44	38.25	71.68	62.56	45.8
	q_{eq} (mg/g)	34.18	52.50	65.04	37.02	68.46	59.54	43.45
	R^2	0.9916	0.9777	0.9646	0.9828	0.9781	0.9663	0.979
	RMSE	0.0291	0.0302	0.0439	0.0309	0.0297	0.0444	0.0321
Nonlinear regression	k_{Th} (mL min^{-1} mg^{-1})	0.383	0.189	0.152	0.309	0.125	0.152	0.269
	q_{Th} (mg/g)	35.00	53.18	64.98	36.89	70.82	59.20	44.99
	q_{eq} (mg/g)	34.18	52.50	65.04	37.02	68.46	59.54	43.45
	R^2	0.9979	0.9956	0.9963	0.9966	0.9968	0.9955	0.9984
	RMSE	0.0181	0.0236	0.0238	0.0223	0.0202	0.0260	0.0151

3.6.3. Yoon-Nelson model

Yoon-Nelson model in linear form was applied to the column data as depicted in Fig. 6 as the plot of ln $[C_t/(C_i - C_t)]$ vs. t and obtained model parameters, k_{YN} from slope and τ from intercept of curve represented in Fig. 6 and R^2 values are given in Table 4 along with the obtained model parameters using nonlinear regression. The obtained values of τ using both regressions were found to be higher at higher values of bed depths whereas lower values of τ were observed for higher values of flow rate and influent concentration. Increase in τ values with depth of the bed can be attributed to availability of more biosorbent for fixed amount of dye and hence τ values increased. Similar trend of higher values of τ at increased bed depths was earlier reported for Acid Yellow 17 adsorption on Tamarind seed based adsorbent [63]. It can also be seen from Table 4 that values of k_{YN} using both regressions increased with increase in C_i values, attributed to increased mass transfer at higher C_i values, leading to increase in k_{YN} values [64]. R^2 values obtained using linear regression (average value of 0.9772) and nonlinear regression (average value of 0.9967) of Yoon-Nelson model were also found to be quite close to unity. R^2 values obtained using nonlinear regressions were found to be quite closer to unity in comparison with linear regression similar to that observed for the Thomas model fitting. Time required for 50% breakthrough obtained experimentally ($t_{0.5}$) and calculated by Yoon-Nelson model (τ) were also found to be close for all the studied column parameters. Again the $t_{0.5}$ and τ values were found to be comparatively closer to each other for nonlinear regression than linear regression. Error values calculated for the Yoon-Nelson model were also very less as seen from Table 4. All these findings confirmed that obtained column data well fitted to the Yoon-Nelson model. Similar trend and fitting of Yoon-Nelson model was reported for Congo red removal using modified clay [65].

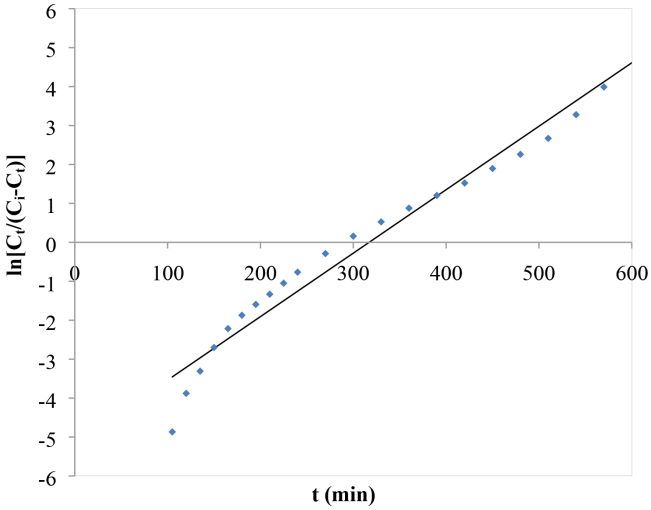

Fig. 6. Yoon-Nelson plot for the removal of Acid Blue 113 dye using SMPD biosorbent (H = 4 cm, C_i = 100 mg/L, F = 6 mL/min).

3.6.4. Comparison of model fitting to the breakthrough data

Best fitting of the applied models to the experimental data has been confirmed by comparing the established breakthrough data (experimental values of C_t/C_i) with the predicted values from the models obtained using nonlinear regression as per the plot shown in Fig. 7. It can be observed from Fig. 7 that experimental values of C_t/C_i are very much closer to C_t/C_i values obtained using Yoon-Nelson and Thomas model whereas values obtained using Adam Bohart model are found to be deviating significantly from the experimental values. The obtained finding from Fig. 7 in addition to R^2 and error values confirmed that Yoon Nelson and Thomas models are in good agreement with the reported breakthrough data.

3.7. Desorption of dye and re-usability of biosorbent

Commercial application of the adsorption is based on re-usability of used adsorbent and application in multiple cycles for dye removal. Re-usability study was performed with SMPD biosorbent being treated using ethanol as the

Table 4
Yoon-Nelson model parameters for the removal of Acid Blue 113 dye using SMPD

Column parameters	H (cm)	3	4	5	4	4	4	4
	C_i (mg/L)	100	100	100	50	200	100	100
	F (mL/min)	8	8	8	8	8	6	10
Linear regression	k_{YN} (min^{-1})	0.0352	0.0213	0.0168	0.0158	0.0282	0.0163	0.0316
	$t_{0.5}$ (min)	95	205	300	270	135	290	135
	τ (min)	103.84	202.05	325.09	290.69	136.20	316.96	139.22
	R^2	0.9916	0.9777	0.9646	0.9828	0.9781	0.9663	0.979
	RMSE	0.0291	0.0302	0.0439	0.0309	0.0297	0.0444	0.0321
Nonlinear regression	k_{YN} (min^{-1})	0.0383	0.0189	0.0152	0.0155	0.0251	0.0152	0.0269
	$t_{0.5}$ (min)	95	205	300	270	135	290	135
	τ (min)	99.75	202.09	308.66	280.39	134.56	299.93	136.76
	R^2	0.9979	0.9956	0.9963	0.9966	0.9968	0.9955	0.9984
	RMSE	0.0181	0.0236	0.0238	0.0223	0.0202	0.0260	0.0151

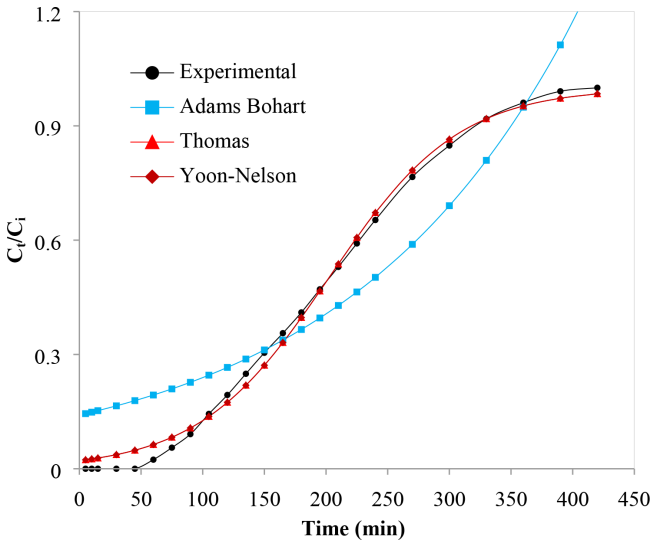

Fig. 7. Comparison of experimental data with the model predicted values for removal of Acid Blue 113 using SMPD (H = 4 cm, C_i = 100 mg/L, F = 8 mL/min).

desorbing agent and subsequently reused in the adsorption performed in the column loaded at 4 cm bed depth and Acid Blue 113 dye solution with 100 mg/L as the influent concentration being passed through the column at 8 mL/min as the constant flow rate. In the desorption operation, ethanol was passed through the dye loaded SMPD biosorbent in the column at 8 mL/min of flow rate and desorption experiments were conducted for 90–100 min. In cycles of elution, maximum desorption of dye (high concentration of dye detected at the outlet) occurred in initial period of elution operation and desorption was very less in later period of operation. The established results for the final extent of desorption of dye and the biosorption capacity during the subsequent re-usability of the biosorbent are shown in Fig. 8. It was observed that the biosorption capacity decreased from 52.5 mg/g for 1st cycle of reuse to 49.42 mg/g for 3rd cycle of re-usability. Extent of desorption (%) was also found to decrease from 98.59% for first cycle to 83.81% for third cycle. Drop

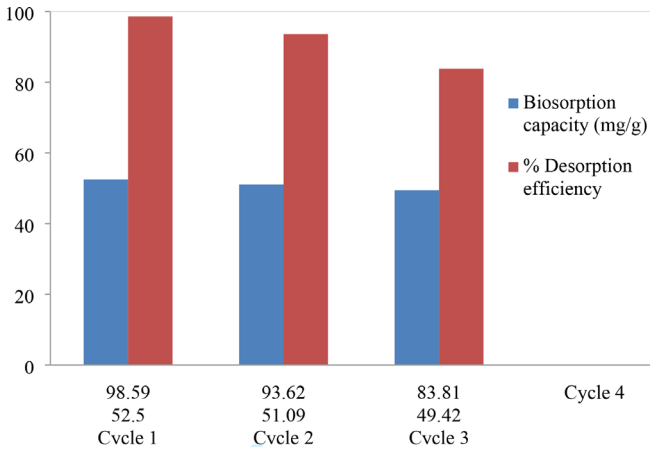

Fig. 8. Re-usability study of SMPD biosorbent for removal of Acid Blue 113 in column operation.

in desorption was obtained as around 15% whereas drop in biosorption capacity was obtained as around 6% after third cycle. The established results in the present work confirmed that adsorbed dye on SMPD biosorbent could be desorbed and recovered biosorbent could be subjected to Acid Blue 113 adsorption again for 3 cycles with some loss in the activity, which is manageable based on using makeup adsorbent.

4. Conclusions

The present study involved application of NaOH and surfactant activated biosorbent obtained from the sustainable biomass of *Prunus dulcis* for Acid Blue 113 removal from wastewater in fixed bed operation. The established results demonstrated the importance of NaOH and cationic surfactant activation based on the enhanced adsorption of anionic, azo dye on the modified biosorbent. Dye removal was facilitated using the waste biomass of *Prunus Dulcis*, which is available in abundant quantity and again at no cost in comparison with the costlier activated carbon. The obtained findings established better performance at higher bed depths and lower values of flow rate. Interference of other compounds as salt possibly present in the real effluent on individual dye removal was also investigated and it was demonstrated that only marginal reduction in removal of dye is obtained. Desorption of dye performed using ethanol and subsequent re-usability of recovered SMPD proved the potential of synthesized biosorbent for dye removal in multiple cycles in comparison with the activated carbon which suffers with regeneration difficulties. All these factors established sustainability of the studied adsorption process from environmental point of view. Overall, the conducted column study confirmed that synthesized SMPD biosorbent is suitable for Acid Blue 113 removal from dye effluent in continuous mode of operation.

Acknowledgements

The authors acknowledge University Grant Commission for assistance under UGC Networking Resource Centre, at the Institute of Chemical Technology, Mumbai, India.

References

[1] X. Li, Z. Wang, J. Ning, M. Gao, W. Jiang, Z. Zhou, G. Li, Preparation and characterization of a novel polyethyleneimine cation-modified persimmon tannin bioadsorbent for anionic dye adsorption, J. Environ. Manage., 217 (2018) 305–314.
[2] J. Huang, S. Chu, J. Chen, Y. Chen, Z. Xie, Enhanced reduction of an azo dye using henna plant biomass as a solid-phase electron donor, carbon source, and redox mediator, Bioresour. Technol., 161 (2014) 465–468.
[3] M.H. Vijaykumar, P.A. Vaishampayan, Y.S. Shouche, T.B. Karegoudar, Decolourization of naphthalene-containing sulfonated azo dyes by Kerstersia sp. strain VKY1, Enzyme Microb. Technol., 40 (2007) 204–211.
[4] K. Vikrant, B.S. Giri, N. Raza, K. Roy, K.-H. Kim, B.N. Rai, R.S. Singh, Recent advancements in bioremediation of dye: Current status and challenges, Bioresour. Technol., 253 (2018) 355–367.
[5] H.M. Pinheiro, E. Touraud, O. Thomas, Aromatic amines from azo dye reduction: status review with emphasis on direct UV spectrophotometric detection in textile industry waste waters, Dye Pigment., 61 (2004) 121–139.

[6] B. Tanhaei, A. Ayati, M. Lahtinen, M. Sillanpää, Preparation and characterization of a novel chitosan/Al_2O_3/magnetite nanoparticles composite adsorbent for kinetic, thermodynamic and isotherm studies of methyl orange adsorption, Chem. Eng. J., 259 (2015) 1–10.
[7] Y. Pan, Y. Wang, A. Zhou, A. Wang, Z. Wu, L. Lv, X. Li, K. Zhang, T. Zhu, Removal of azo dye in an up-flow membrane-less bio-electrochemical system integrated with bio-contact oxidation reactor, Chem. Eng. J., 326 (2017) 454–461.
[8] M. Fatima, R. Farooq, R.W. Lindström, M. Saeed, A review on biocatalytic decomposition of azo dyes and electrons recovery, J. Mol. Liq., 246 (2017) 275–281.
[9] M. Shirzad-Siboni, S.J. Javad, O. Giahi, I. Kim, S. Lee, J. Yang, Removal of acid blue 113 and reactive black 5 dye from aqueous solutions by activated red mud, J. Ind. Eng. Chem., 20 (2014) 1432–1437.
[10] X. Li, T. Wang, G. Qu, D. Liang, S. Hu, Enhanced degradation of azo dye in wastewater by pulsed discharge, J. Environ. Manage., 172 (2016) 186–192.
[11] S. Mozia, A.W. Morawski, M. Toyoda, T. Tsumura, Integration of photo catalysis and membrane distillation for removal of mono- and poly-azo dyes from water, Desalination, 250 (2010) 666–672.
[12] A. Szyguła, E. Guibal, M. Ruiz, A.M. Sastre, The removal of sulphonated azo-dyes by coagulation with chitosan, Colloids Surfaces A Physicochem. Eng. Asp., 330 (2008) 219–226.
[13] C. Tizaoui, N. Grima, Kinetics of the ozone oxidation of reactive orange 16 azo-dye in aqueous solution, Chem. Eng. J., 173 (2011) 463–473.
[14] C. Liu, H. Mao, J. Zheng, S. Zhang, Tight ultra filtration membrane: Preparation and characterization of thermally resistant carboxylated cardo poly (arylene ether ketone)s (PAEK-COOH) tight ultra filtration membrane for dye removal, J. Membr. Sci., 530 (2017) 1–10.
[15] M.M. Ghoneim, H.S. El-desoky, N.M. Zidan, Electro-Fenton oxidation of sunset yellow FCF azo-dye in aqueous solutions, Desalination, 274 (2011) 22–30.
[16] S. Song, J. Fan, Z. He, L. Zhan, Z. Liu, J. Chen, X. Xu, Electrochimica acta electrochemical degradation of azo dye C.I. Reactive Red 195 by anodic oxidation on Ti/SnO_2 – Sb /PbO_2 electrodes, Electrochim. Acta, 55 (2010) 3606–3613.
[17] S.N. Jain, P.R. Gogate, NaOH-treated dead leaves of Ficus racemosa as an efficient biosorbent for Acid Blue 25 removal, Int. J. Environ. Sci. Technol., 14 (2017) 531–542.
[18] G. Crini, Non-conventional low-cost adsorbents for dye removal: A review, Bioresour. Technol., 97 (2006) 1061–1085.
[19] K.B. Tan, M. Vakili, B.A. Horri, P.E. Poh, A.Z. Abdullah, B. Salamatinia, Adsorption of dyes by nanomaterials: Recent developments and adsorption mechanisms, Sep. Purif. Technol., 150 (2015) 229–242.
[20] A. Salima, B. Benaouda, B. Noureddine, L. Duclaux, Application of Ulva lactuca and Systoceira stricta algae-based activated carbons to hazardous cationic dyes removal from industrial effluents, Water Res., 47 (2013) 3375–3388.
[21] J. Ooi, L.Y. Lee, B.Y.Z. Hiew, S.T.- Gopakumar, S.S. Lim, S. Gan, Assessment of fish scales waste as a low cost and eco-friendly adsorbent for removal of an azo dye: Equilibrium, kinetic and thermodynamic studies, Bioresour. Technol., 245 (2017) 656–664.
[22] L.Y. Lee, S. Gan, M.S.Y. Tan, S.S. Lim, X.J. Lee, Y.F. Lam, Effective removal of Acid Blue 113 dye using overripe Cucumis sativus peel as an eco-friendly biosorbent from agricultural residue, J. Clean. Prod., 113 (2016) 194–203.
[23] L.Y. Lee, D.Z.B. Chin, X.J. Lee, N. Chemmangattuvalappil, S. Gan, Evaluation of Abelmoschus esculentus (lady's finger) seed as a novel biosorbent for the removal of Acid Blue 113 dye from aqueous solutions, Process Saf. Environ. Prot., 94 (2014) 329–338.
[24] M. Shaban, M.R. Abukhadra, A.A.P. Khan, B.M. Jibali, Removal of Congo red, methylene blue and Cr(VI) ions from water using natural serpentine, J. Taiwan Inst. Chem. Eng., 82 (2018) 102–116.
[25] S. Li, J. Zhang, S. Jamil, Q. Cai, S. Zang, Conversion of eggshells into calcium titanate cuboid and its adsorption properties, Res. Chem. Intermed., 44 (2018) 3933–3946.
[26] E. Gengec, U. Ozdemir, B. Ozbay, I. Ozbay, S. Veli, Optimizing dye adsorption onto a waste-derived (modified charcoal ash) adsorbent using Box – Behnken and central composite design procedures, Water Air Soil Pollut., 224 (2013) 1–12. doi:10.1007/s11270-013-1751-6.
[27] R.S. Aliabadi, N.O. Mahmoodi, Synthesis and characterization of polypyrrole, polyaniline nanoparticles and their nanocomposite for removal of azo dyes; sunset yellow and Congo red, J. Clean. Prod., 179 (2018) 235–245.
[28] H. Sayğılı, F. Güzel, Performance of new mesoporous carbon sorbent prepared from grape industrial processing wastes for malachite green and congo red removal, Chem. Eng. Res. Des., 100 (2015) 27–38.
[29] S.N. Jain, P.R. Gogate, Acid Blue 113 removal from aqueous solution using novel biosorbent based on NaOH treated and surfactant modified fallen leaves of Prunus Dulcis, J. Environ. Chem. Eng., 5 (2017) 3384–3394.
[30] N. Wang, X. Xu, L. Yang, L. Yuan, T. Xiao, H. Li, H. Yu, Plate column adsorption of Pb(II) from industrial wastewater on sponge-type composite adsorbent: Optimization and application, J. Ind. Eng. Chem., (2018). doi:10.1016/j.jiec.2018.05.048.
[31] E. Oguz, Fixed-bed column studies on the removal of Fe^{3+} and neural network modelling, Arab. J. Chem., 10 (2017) 313–320.
[32] J.B. Modak, A. Bhowal, S. Datta, Experimental study and mathematical modeling of breakthrough curve in rotating packed bed, Chem. Eng. Process. Process Intensif., 99 (2016) 19–24.
[33] V.K. Gupta, B. Gupta, A. Rastogi, S. Agarwal, A. Nayak, A comparative investigation on adsorption performances of mesoporous activated carbon prepared from waste rubber tire and activated carbon for a hazardous azo dye — Acid Blue 113, J. Hazard. Mater., 186 (2011) 891–901.
[34] M. Yusuf, M.A. Khan, M. Otero, E.C. Abdullah, M. Hosomi, A. Terada, S. Riya, Synthesis of CTAB intercalated graphene and its application for the adsorption of AR265 and AO7 dyes from water, J. Colloid Interf. Sci., 493 (2017) 51–61.
[35] M. Baghdadi, B.A. Soltani, M. Nourani, Malachite green removal from aqueous solutions using fibrous cellulose sulfate prepared from medical cotton waste: Comprehensive batch and column studies, J. Ind. Eng. Chem., 55 (2017) 128–139.
[36] S.N. Jain, P.R. Gogate, Fixed bed column study for the removal of Acid Blue 25 dye using NaOH-treated fallen leaves of Ficus racemosa, Desal. Water Treat., 85 (2017) 215–225.
[37] Y.-Z. Yan, Q.-D. An, Z.-Y. Xiao, S.-R. Zhai, B. Zhai, Z. Shi, Interior multi-cavities/surface engineering of alginate hydrogels with PEI for exceptionally efficient chromium removal in batch and continuous aqueous systems, J. Mater. Chem. A., 5 (2017) 17073–17087.
[38] M.L.G. Vieira, M.S. Martinez, G.B. Santos, G.L. Dotto, L.A.A. Pinto, Azo dyes adsorption in fixed bed column packed with different deacetylation degrees chitosan coated glass beads Authors:, J. Environ. Chem. Eng., 6 (2018) 3233–3241.
[39] A.P. Lim, A.Z. Aris, Continuous fixed-bed column study and adsorption modeling: Removal of cadmium (II) and lead (II) ions in aqueous solution by dead calcareous skeletons, Bio-Chem. Eng. J., 87 (2014) 50–61.
[40] M. Jafari, M.R. Rahimi, M. Ghaedi, H. Javadian, A. Asfaram, Fixed-bed column performances of azure-II and auramine-O adsorption by Pinus eldarica stalks activated carbon and its composite with ZnO nanoparticles: optimization by response surface methodology based on central composite design, J. Colloid Interf. Sci., 507 (2017) 172–189.
[41] S.N. Jain, P.R. Gogate, Adsorptive removal of acid violet 17 dye from wastewater using biosorbent obtained from NaOH and H_2SO_4 activation of fallen leaves of Ficus racemosa, J. Mol. Liq., 243 (2017) 132–143.
[42] G.S. Bohart, E.Q. Adams, Some aspects of the behavior of charcoal with respect to chlorine, J. Am. Chem. Soc., 42 (1920) 523–544.

[43] H.C. Thomas, Heterogeneous ion exchange in a flowing system, J. Am. Chem. Soc., 66 (1944) 1664–1666.
[44] Y.H. Yoon, J.H. Nelson, Application of gas adsorption kinetics I. A theoretical model for respirator cartridge service life, Am. Ind. Hyg. Assoc. J., 45 (1984) 509–516.
[45] M. Dastkhoon, M. Ghaedi, A. Asfaram, M.H.A. Azqhandi, S. Hajati, M.K. Purkait, Simultaneous removal of dyes onto nanowires adsorbent use of ultrasound assisted adsorption to clean waste water: Chemometrics for modeling and optimization, multicomponent adsorption and kinetic study, Chem. Eng. Res. Des., 124 (2017) 222–237.
[46] B. Zhao, Y. Shang, W. Xiao, C. Dou, R. Han, Adsorption of Congo red from solution using cationic surfactant modified wheat straw in column model, J. Environ. Chem. Eng., 2 (2014) 40–45.
[47] X. Xu, B. Gao, X. Tan, X. Zhang, Q. Yue, Y. Wang, Q. Li, Nitrate adsorption by stratified wheat straw resin in lab-scale columns, Chem. Eng. J., 226 (2013) 1–6.
[48] T.V.N. Padmesh, K. Vijayaraghavan, G. Sekaran, M. Velan, Application of Azolla rongpong on biosorption of acid red 88, acid green 3, acid orange 7 and acid blue 15 from synthetic solutions, Chem. Eng. J., 122 (2006) 55–63.
[49] M. Nainamalai, M. Palani, B. Soundarajan, A.E. J.S.S, Decolorization of synthetic dye wastewater using packed bed electro-adsorption column, Chem. Eng. Process. Process Intensif., 130 (2018) 160–168.
[50] E. Khoo, S. Ong, S. Ha, Removal of basic dyes from aqueous environment in single and binary systems by sugarcane bagasse in a fixed-bed column, Desal. Water Treat., 37 (2012) 215–222.
[51] N. Saranya, A. Ajmani, V. Sivasubramanian, N. Selvaraju, Hexavalent chromium removal from simulated and real effluents using Artocarpus heterophyllus peel biosorbent-Batch and continuous studies, J. Mol. Liq., 265 (2018) 779–790.
[52] H. Kalavathy, B. Karthik, L.R. Miranda, Removal and recovery of Ni and Zn from aqueous solution using activated carbon from Hevea brasiliensis: Batch and column studies, Colloids Surfaces B. Biointerfaces, 78 (2010) 291–302.
[53] R. Lakshmipathy, N.C. Sarada, Methylene blue adsorption onto native watermelon rind: batch and fixed bed column studies, Desal. Water Treat., 57 (2016) 10632–10645.
[54] L. Sheng, Y. Zhang, F. Tang, S. Liu, Mesoporous/microporous silica materials: Preparation from natural sands and highly efficient fixed-bed adsorption of methylene blue in waste water, Microporous Mesoporous Mater., 257 (2018) 9–18.
[55] P.B. Bhakat, A.K. Gupta, S. Ayoob, Feasibility analysis of As(III) removal in a continuous flow fixed bed system by modified calcined bauxite (MCB), J. Hazard. Mater., 139 (2007) 286–292.
[56] S.N. Jain, P.R. Gogate, Efficient removal of Acid Green 25 dye from wastewater using activated Prunus Dulcis as biosorbent: Batch and column studies, J. Environ. Manage., 210 (2018) 226–238.
[57] R. Han, Y. Wang, W. Yu, W. Zou, J. Shi, H. Liu, Biosorption of methylene blue from aqueous solution by rice husk in a fixed-bed column, J. Hazard. Mater., 141 (2007) 713–718.
[58] B. Li, Q. Wang, J. Guo, W. Huan, L. Liu, Sorption of methyl orange from aqueous solution by protonated amine modified hydrochar, Bioresour. Technol., 268 (2018) 454–459.
[59] R. Han, Y. Wang, X. Zhao, Y. Wang, F. Xie, J. Cheng, M. Tang, Adsorption of methylene blue by phoenix tree leaf powder in a fixed-bed column: experiments and prediction of breakthrough curves, Desalination, 245 (2009) 284–297.
[60] E. Gutiérrez-Segura, A. Colín-Cruz, M. Solache-Ríos, C. Fall, Removal of denim blue from aqueous solutions by inorganic adsorbents in a fixed-bed column, Water Air Soil Pollut., 223 (2012) 5505–5513.
[61] S. Afroze, T.K. Sen, H.M. Ang, Adsorption performance of continuous fixed bed column for the removal of methylene blue (MB) dye using Eucalyptus sheathiana bark biomass, Res. Chem. Intermed., 42 (2016) 2343–2364.
[62] V. Dulman, S.-M. Cucu-Man, I. Bunia, M. Dumitras, Batch and fixed bed column studies on removal of Orange G acid dye by a weak base functionalized polymer, Desal. Water Treat., 57 (2016) 14708–14727.
[63] H. Patel, R.T. Vashi, Fixed bed column adsorption of Acid yellow 17 dye onto tamarind seed powder, Can. J. Chem. Eng., 90 (2012) 180–185.
[64] Y. Zhang, J. Li, W. Li, Effect of particle size on removal of sunset yellow from aqueous solution by chitosan modified diatomite in a fixed bed column, RSC Adv., 5 (2015) 85673–85681.
[65] S. Vahidhabanu, D. Karuppasamy, A.I. Adeogun, B.R. Babu, Impregnation of zinc oxide modified clay over alginate beads: a novel material for the effective removal of congo red from wastewater, RSC Adv., 7 (2017) 5669–5678.